



0957-4166(95)00098-4

## Synthesis and Stereochemistry of Optically Active Biliverdin Cyclic Esters

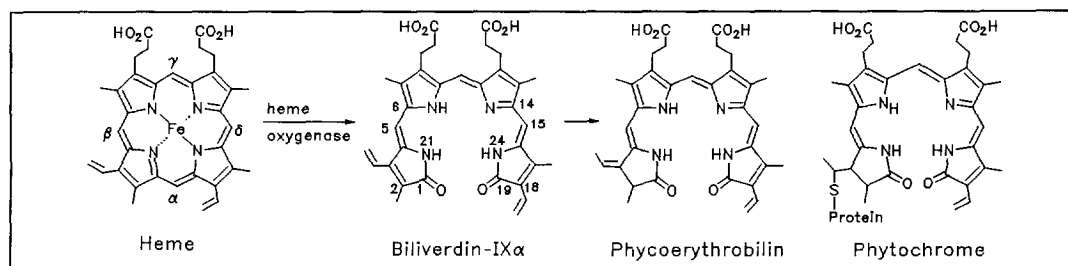
Stefan E. Boiadjiev, D. Timothy Anstine and David A. Lightner\*

Department of Chemistry, University of Nevada, Reno, Nevada 89557-0020 USA

**Abstract:** ( $\beta S, \beta' S$ )-Dimethylmesobiliverdin-XIII $\alpha$  dimethyl ester exhibits a positive long wavelength circular dichroism Cotton effect ( $\Delta\epsilon_{644}^{\max} = +6.1$ ) in  $\text{CHCl}_3$ , indicating an excess of the *P*-helical conformation of the pigment. But when the pigment's propionic acids are linked together by  $-(\text{CH}_2)_n-$  chains in *cyclic esters*, the choice of cyclic ester conformation and pigment helicity is governed by the number ( $n$ ) of  $\text{CH}_2$  units, with  $\Delta\epsilon$  near 640 nm varying from positive when  $n=1, 5$  and 6, to negative when  $n=2, 3$  and 4.

### INTRODUCTION

Biliverdin-IX $\alpha$  is a blue-green pigment formed in plant and animal metabolism by oxidative cleavage of the porphyrin macrocycle of heme.<sup>1,2,3</sup> In mammals biliverdin is reduced rapidly and efficiently to bilirubin, the yellow pigment of jaundice, which is eliminated in normal metabolism following esterification in the liver by a glucuronosyl transferase and excretion into bile.<sup>1,4</sup> In other animals, biliverdin is excreted directly.<sup>1</sup> Verdins are distributed widely in nature. They serve as a colorant in egg shells, bones and butterfly wings, and are found, *mutatis mutandis*, in plants.<sup>1-3</sup> In blue-green algae, biliverdin is converted into photosynthetic pigments, phycocyanobilin and phycoerythrobilin.<sup>2,3</sup> In higher plants and some algae, it is converted into phytochrome, which is the photosensory pigment mediating photomorphogenesis.<sup>2,3</sup> Although four different biliverdins might be formed *via* oxidative cleavage of heme at the  $\alpha$ ,  $\beta$ ,  $\gamma$  or  $\delta$  site, typically the  $\alpha$ -carbon is excised to give biliverdin-IX $\alpha$ , which is the most common biliverdin type.<sup>1,2</sup>



The constitutional structure of biliverdin was determined long ago by total synthesis,<sup>5</sup> and its stereochemistry is straightforward. In its most stable conformation, biliverdin adopts a helical, lock-washer shape

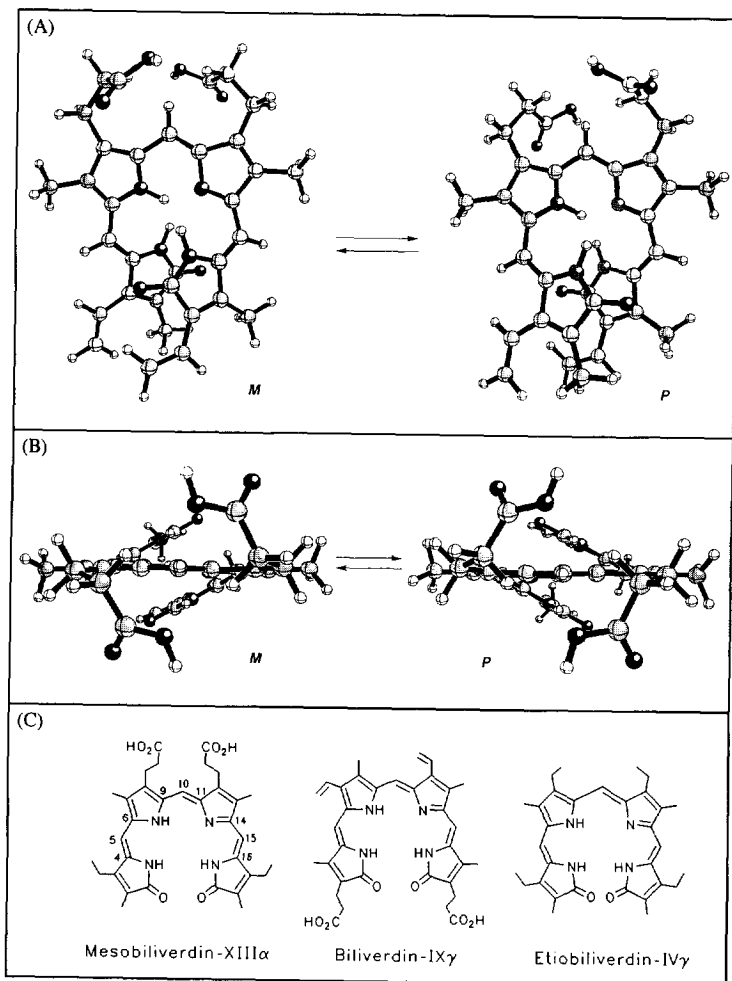


**FIGURE 1.** Ball and stick conformational representations for interconverting helical enantiomers of biliverdin-IX $\alpha$ . *M* corresponds to a left-handed or (-)-helix; *P* to a right-handed or (+)-helix. (A) Face view. (B) Edge view looking from C(10) through the molecule. (C) Porphyrin-like representations for biliverdin analogs that adopt the helical conformations of (A) and (B).

verdin helix is more evenly distributed than that found by molecular dynamics, which places most of the dissymmetry in the dipyrnone components.

The barrier to interconverting *M* and *P* helical verdin conformers is relatively low ( $\Delta G_{200\text{K}}^{\ddagger} \approx 10$  kcal/mole)<sup>8</sup> but is raised to  $\Delta G_{333\text{K}}^{\ddagger} \approx 25$  kcal/mole by connecting the N(21) and N(24) nitrogens with a -CH<sub>2</sub>- bridge (Fig. 2A).<sup>2,9</sup> Although the *M*  $\rightleftharpoons$  *P* interconversion is thus slowed sufficiently to permit separation of the *M* and *P* enantiomers, the bridge distorts the verdin helix, with the C(4)=C(5), C(5)-C(6), C(9)-C(10), C(10)=C(11), C(14)-C(15) and C(15)=C(16) torsion angles of 8.9, 34.2, -47.2, -2.5, 13.7 and 8.5 degrees, respectively, found in molecular dynamics calculations<sup>7</sup> and the helix pitch lowering to 2.6 Å for the O(1) to O(19) distance.<sup>2,7</sup> Other verdins with high *M*  $\rightleftharpoons$  *P* interconversion barriers ( $\Delta G_{293}^{\ddagger} \approx 21$ -24 kcal/mole)<sup>10</sup> have been prepared by linking ring carbons 2 and 18 through a four carbon bridge (Fig 2B).

(Fig. 1A and B).<sup>2,6</sup> The helical shape is generally independent of the location and nature of the pyrrole  $\beta$ -substituents. Biliverdin-IX $\alpha$  and mesobiliverdin-XIII $\alpha$  (Fig. 1C), their esters and analogs with propionic acids relocated (*e.g.*, biliverdin-IX $\gamma$ , Fig. 1C), as well as analogs with only alkyl groups (*e.g.*, etiobiliverdin-IV $\gamma$ , Fig. 1C) adopt essentially the same conformation: either a left-handed (*M*) or a right-handed (*P*) helix (Figs. 1A and B). In crystals of biliverdin-IX $\alpha$  dimethyl ester the torsion angles about C(4)=C(5), C(5)-C(6), C(9)-C(10), C(10)=C(11), C(14)-C(15) and C(15)=C(16) are 6.5, 11.8, 9.6, 2.0, 18.5 and 3.2 degrees, respectively.<sup>2,6a</sup> And the pitch of the helix, as measured by the O(1) to O(19) vertical distance is not large, 3.34Å. The torsion angles are similar to those found in molecular dynamics calculations<sup>7</sup> on mesobiliverdin-XIII $\alpha$  dimethyl ester, 3.5, 27.2, 4.8, 1.9, 26.6 and 3.7 degrees, respectively, where the pitch of the helix is nearly the same, 3.0 Å. In the crystal, the turn of the

Such bridged verdins have been resolved into *M* and *P* helical conformers, but here the verdin helix is relatively undistorted compared with mesobiliverdin-XIII $\alpha$  dimethyl ester and has C(4)=C(5), C(5)-C(6), C(9)-C(10), C(10)=C(11), C(14)-C(15) and C(15)=C(16) torsion angles of 5.2, 31.6, 0.9, 1.8, 28.8 and 3.4 degrees, respectively, and a pitch of 2.8 Å for the O(1) to O(19) vertical distance as found by molecular dynamics.<sup>7</sup> Most recently, cyclic esters of mesobiliverdin-IX $\alpha$  were prepared with propionic acid groups linked by  $-(\text{CH}_2)_n-$  units (Fig. 2C), with  $n=1, 3$  and  $4$ .<sup>11</sup> No apparent distortion of the verdin helix was detected; however, little is known of their stereochemistry.

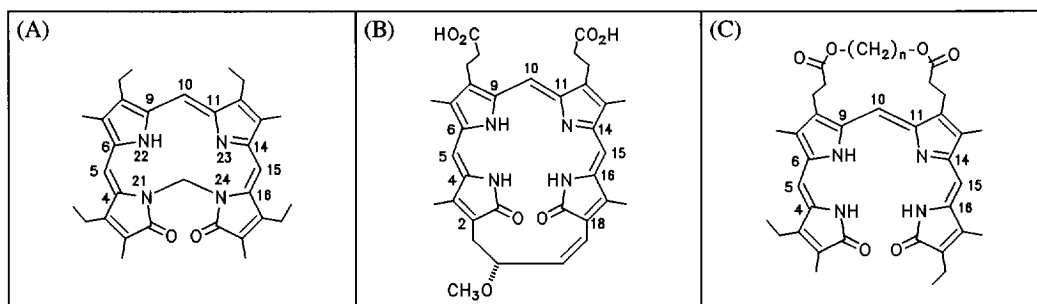
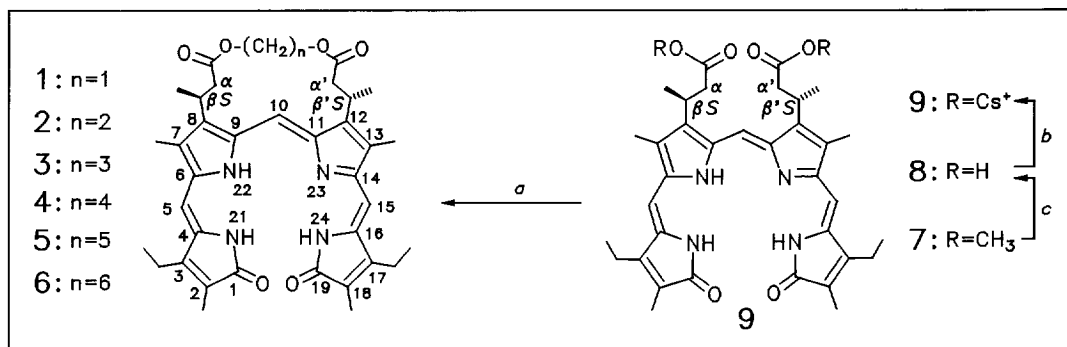


**FIGURE 2.** Porphyrin-like representations for (A) etiobiliverdin-IV $\gamma$  with N(21) and N(24) linked by a  $-\text{CH}_2-$  group (ref. 9), (B) biliverdin-III $\alpha$  with erstwhile vinyl groups linked so as to form a 4-carbon bridge between C(2) and C(18) (ref. 10b), and (C) cyclic esters of mesobiliverdin-IX $\alpha$  (ref. 11), with  $n=1, 3$  or  $4$ .

Interestingly, the *M*  $\rightleftharpoons$  *P* conformational equilibrium in unbridged verdins (Fig. 1A) may be tilted toward the *M* or the *P* helix as in the biliverdin-IX $\gamma$  (Fig. 1C) found in the bilin binding protein from *Pieris brassicae*<sup>2,12</sup> or by covalently attaching a chiral group, as in biliverdin-IX $\alpha$  derivatized as amides with optically active amino acid esters or tripeptide esters.<sup>13</sup> At present, however, ( $\beta S, \beta' S$ )-dimethylmesobiliverdin-XIII $\alpha$  (**8**) or its dimethyl ester (**7**) constitutes the first examples where the stereogenic centers are located in the propionic acid groups. In the current work, we use circular dichroism (CD) spectroscopy to evaluate the influence of such stereogenic centers on the *M*  $\rightleftharpoons$  *P* verdin conformational equilibrium and explicate the stereochemistry and unexpectedly varying CD spectra of the cyclic esters (**1-6**) of (**8**).

### Synthetic Scheme



<sup>a</sup>  $\text{X}(\text{CH}_2)_n\text{X}/(\text{CH}_3)_2\text{SO}$  ( $\text{X}=\text{I}$  for  $n=1$ ; otherwise,  $\text{X}=\text{Br}$ ). <sup>b</sup>  $\text{Cs}_2\text{CO}_3/\text{THF}-\text{CH}_3\text{OH}$ . <sup>c</sup>  $\text{NaOH}/\text{THF}-\text{CH}_3\text{OH}$ ; then  $\text{HCl}$ .

## RESULTS AND DISCUSSION

**Synthesis.** ( $\beta S, \beta' S$ )-Dimethylmesobiliverdin-XIII $\alpha$  dimethyl ester (**7**) was prepared as described previously<sup>14</sup> and saponified smoothly with NaOH in aqueous tetrahydrofuran at 50°C to give diacid **8** in 92% isolated yield. The dicesium salt (**9**) of **8** was prepared from Cs<sub>2</sub>CO<sub>3</sub> and converted to cyclic esters **1-6**, typically in >62% yield by using a five-fold excess of  $\alpha, \omega$ -dihaloalkane. This represents an improvement over the procedure recently reported<sup>11</sup> for the methylene and cyclic esters of biliverdin-IX $\alpha$  and mesobiliverdin-IX $\alpha$ .

**NMR Spectra.** The <sup>13</sup>C-NMR spectra of **1-6** (Table 1) are consistent with a ( $\beta S, \beta' S$ )-dimethylmesobiliverdin-XIII $\alpha$  structure having propionic acids linked with  $-(CH_2)_n-$  belts to form cyclic esters. Although the data are very similar to those of the dimethyl ester (**7**),<sup>14</sup> the OCH<sub>3</sub> quartet of **7** is missing in **1-6**, having been replaced by an -OCH<sub>2</sub>- triplet (**1-6**). Esters **3-6** have additional triplets from the ester belts: -OCH<sub>2</sub>CH<sub>2</sub>- (**3** and **4**) and -OCH<sub>2</sub>CH<sub>2</sub>CH<sub>2</sub>- (**5** and **6**). Long range influence from the cyclic ester belts shows up at the C(5/15) =CH- resonance, which is most deshielded in **1** (with the smallest belt). Interestingly, the C(7)/C(13) methyls are slightly more shielded in the smaller belted cyclic esters (**1-3**) as compared with the larger (**4-6**) and the acyclic parent (**7**). Probably the greatest long range effect is found at the central C(10) =CH-, which is deshielded in **1** by ~2 ppm relative to **7** (or **2, 3** and **6**) but shielded by ~0.5-1.5 ppm in **4** and **5** relative to **7** (or **2, 3** and **6**).

TABLE 1. <sup>13</sup>C-NMR Spectral Assignments<sup>a</sup> for ( $\beta S, \beta' S$ )-Dimethylmesobiliverdin-XIII $\alpha$  Cyclic Esters (**1-6**) and ( $\beta S, \beta' S$ )-Dimethylmesobiliverdin-XIII $\alpha$  Dimethyl Ester (**7**) in CDCl<sub>3</sub> Solvent at 22°C.

Carbon Resonance	Chemical Shift, $\delta$ (ppm) for						
	1	2	3	4	5	6	7
1,19 -CO	170.0	170.9	171.7	172.2	171.9	172.2	172.02
2,18 -CH <sub>3</sub>	8.25	8.24	8.28	8.32	8.26	8.26	8.29
2,18	128.1	128.0	128.2	128.2	128.3	128.1	128.1
3,17 -CH <sub>2</sub> CH <sub>3</sub>	14.46	14.48	14.46	14.49	14.45	14.46	14.46
3,17 -CH <sub>2</sub> CH <sub>3</sub>	17.86	17.84	17.82	17.85	17.82	17.83	17.87
3,17	146.9	147.0	146.7	146.9	146.7	146.8	146.8
4,16	140.4	140.4	140.0	140.3	140.0	140.1	140.3
5,15 =CH-	96.38	96.13	96.10	96.09	95.99	96.03	96.05
6,14	149.8	149.9	150.1	150.1	150.3	150.0	150.0
7,13 -CH <sub>3</sub>	10.26	10.22	10.11	10.38	10.48	10.30	10.38
7,13	127.4	127.9	127.6	127.5	127.2	127.3	127.3
8,12	139.6	139.4	139.7	139.6	139.8	139.7	139.6
9,11	140.7	140.7	141.0	141.3	141.4	141.7	141.7
10 =CH-	117.5	115.6	115.1	114.6	113.6	115.0	115.0
$\alpha, \alpha'$ -CH <sub>2</sub> -	41.65	40.89	41.53	41.90	42.04	41.94	41.40
$\beta, \beta'$ -CH <sub>3</sub>	19.56	21.45	21.35	20.98	20.18	20.86	21.00
$\beta, \beta'$ -CH-	28.14	28.64	28.47	28.51	28.28	28.16	28.00
-OCH <sub>2</sub> -	80.65	61.85	63.83	63.97	64.27	64.66	51.63
-OCH <sub>2</sub> CH <sub>2</sub> -	—	—	28.18	25.26	28.08	27.83	—
-OCH <sub>2</sub> CH <sub>2</sub> CH <sub>2</sub> -	—	—	—	—	23.48	25.96	—
$\alpha, \alpha'$ -CO	172.5	171.8	172.3	172.2	172.4	172.3	172.6

<sup>a</sup> Chemical shifts ( $\delta$ ) in ppm downfield from (CH<sub>3</sub>)<sub>4</sub>Si.

The  $^1\text{H-NMR}$  spectra of **1-6** (Table 2) are also consistent with the ( $\beta\text{S},\beta'\text{S}$ )-dimethylmesobiliverdin- $\text{XIII}\alpha$  core structure.<sup>14</sup> New signals appear for the various  $\text{CH}_2$  resonances in the cyclic ester  $(\text{CH}_2)_n$  belts. The pyrrole and lactam  $\text{N-Hs}$  are somewhat deshielded in **1** relative to **7** and **3-6**; in **2** they are shielded. The intramolecularly hydrogen bonded pyrrole  $\text{NH}$  is quite broad and somewhat more deshielded in the cyclic esters **1** and **2** than in the acyclic analog (**7**). Interestingly, the propionic acid  $\alpha(\alpha')$  hydrogens are split into an  $\text{ABX}$  pattern in **1-6** but remain a simple doublet in **7**. The data indicate very restricted motion in the cyclic esters, surprising for 14-19 membered (ester) rings, but not in the acyclic (**7**).

**TABLE 2.**  $^1\text{H-NMR}$  Spectral Assignments for ( $\beta\text{S},\beta'\text{S}$ )-Dimethylmesobiliverdin- $\text{XIII}\alpha$  Cyclic Esters and ( $\beta\text{S},\beta'\text{S}$ )-Dimethylmesobiliverdin- $\text{XIII}\alpha$  Dimethyl Ester (**7**) in  $\text{CDCl}_3$  Solvent at  $22^\circ\text{C}$ .

Proton Resonance	Chemical Shift, $\delta$ (ppm) for						
	1	2	3	4	5	6	7
2,18 $-\text{CH}_3$	1.82	1.83	1.82	1.83	1.82	1.83	1.81
3,17 $-\text{CH}_2\text{CH}_3$	1.23 <sup>a</sup>	1.23 <sup>a</sup>	1.22 <sup>a</sup>	1.22 <sup>a</sup>	1.22 <sup>a</sup>	1.23 <sup>a</sup>	1.21 <sup>a</sup>
3,17 $-\text{CH}_2\text{CH}_3$	2.53 <sup>b</sup>	2.54 <sup>b</sup>	2.52 <sup>b</sup>	2.53 <sup>b</sup>	2.52 <sup>b</sup>	2.53 <sup>b</sup>	2.52 <sup>b</sup>
5,15 $-\text{CH}=\text{}$	6.00	6.03	5.95	5.98	5.96	5.98	5.97
7,13 $-\text{CH}_3$	2.16	2.19	2.15	2.17	2.17	2.17	2.16
$\alpha,\alpha'$ $-\text{CH}_2-$	2.68 <sup>c</sup> 2.71 <sup>c</sup>	2.83 <sup>g</sup> 2.90 <sup>g</sup>	2.79 <sup>j</sup> 2.88 <sup>j</sup>	2.74 <sup>m</sup> 2.81 <sup>m</sup>	2.71 <sup>o</sup> 2.73 <sup>o</sup>	2.73 <sup>p</sup> 2.74 <sup>p</sup>	2.73 <sup>q</sup>
$\beta,\beta'$ $-\text{CH}-$	3.50 <sup>d</sup>	3.51 <sup>d</sup>	3.52 <sup>d</sup>	3.55 <sup>d</sup>	3.51 <sup>d</sup>	3.52 <sup>d</sup>	3.54 <sup>d</sup>
$\beta,\beta'$ $-\text{CH}_3$	1.57 <sup>e</sup>	1.45 <sup>h</sup>	1.39 <sup>k</sup>	1.41 <sup>h</sup>	1.39 <sup>k</sup>	1.42 <sup>k</sup>	1.41 <sup>k</sup>
$-\text{OCH}_2-$	5.69 <sup>f</sup>	4.03 <sup>i</sup> 4.15 <sup>i</sup>	4.09 <sup>i</sup> 4.11 <sup>i</sup>	3.97 <sup>i</sup> 4.08 <sup>i</sup>	4.10 <sup>i</sup> 4.17 <sup>i</sup>	4.10 <sup>i</sup>	3.63 <sup>f</sup>
$-\text{OCH}_2\text{CH}_2-$	—	—	1.79 <sup>l</sup>	1.64 <sup>n</sup>	1.57-1.69 <sup>l</sup>	1.16 <sup>l</sup>	—
$-\text{OCH}_2\text{CH}_2\text{CH}_2-$	—	—	—	—	1.57-1.69 <sup>l</sup>	1.44 <sup>l</sup>	—
10 $=\text{CH}-$	6.94	7.02	7.00	6.95	6.89	6.99	6.96
21,24 $-\text{NHCO}$	8.24	7.74	8.02	7.93	8.05	7.91	7.97
22 $-\text{NH}$	11.6	11.9	9.8	10.3	9.9	9.9	11.3

<sup>a</sup> t ( $J=7.6$  Hz); <sup>b</sup> q ( $J=7.6$  Hz); <sup>c</sup>  $\text{ABX}$ , dd ( $J=3.9, 8.8, 13.5$  Hz); <sup>d</sup> m,  $\text{ABX}$ ; <sup>e</sup> d ( $J=7.4$  Hz); <sup>f</sup> s; <sup>g</sup>  $\text{ABX}$ , dd ( $J=5.3, 10.5, 14.9$  Hz); <sup>h</sup> d ( $J=7.2$  Hz); <sup>i</sup> m,  $\text{AA'BB'}$ ; <sup>j</sup>  $\text{ABX}$ , dd ( $J=7.1, 10.2, 14.6$  Hz); <sup>k</sup> d ( $J=7.1$  Hz); <sup>l</sup> br.m; <sup>m</sup>  $\text{ABX}$ , dd ( $J=7.6, 8.3, 14.5$  Hz); <sup>n</sup> very br.t; <sup>o</sup>  $\text{ABX}$ , dd ( $J=1.4, 4.1, 11.8$  Hz); <sup>p</sup>  $\text{ABX}$ , dd ( $J=7.4, 8.2, 15.3$  Hz); <sup>q</sup> d ( $J=7.6$  Hz); <sup>r</sup> s,  $\text{OCH}_3$ .

**UV-Vis and CD Spectra.** The presence of the cyclic ester appears to exert no special influence on the UV-vis spectra of **1-6** as compared with the acyclic analog **7** (Table 3). The spectra of **1-6** and **7** are nearly invariant in  $\text{CHCl}_3$  and  $\text{CH}_3\text{OH}$  solvents, with long wavelength absorption maxima near 640 nm ( $\epsilon \sim 14,000$ ) and more intense shorter wavelength absorption maxima near 370 nm ( $\epsilon \sim 50,000$ ) and 305 nm ( $\epsilon \sim 22,000$ ). In contrast, the CD spectra differ. In both solvents, the parent acyclic ester **7** exhibits a positive Cotton effect (CE) for the long wavelength CD transition near 640 nm, a more intense negative CE for the  $\sim 365$  nm transition, and a weaker positive transition for the  $\sim 300$  nm transition. Tying the propionic acids together in cyclic esters causes only minor variations in the CE magnitudes for the shortest ( $-\text{CH}_2-$ ) and longest ( $-(\text{CH}_2)_5-$  and  $-(\text{CH}_2)_6-$ ) belts in **1, 5** and **6**, respectively. But tying them with intermediate length belts ( $-(\text{CH}_2)_2-$ ,  $-(\text{CH}_2)_3-$  and  $-(\text{CH}_2)_4-$ ), **2, 3** and **4**, respectively, causes CE sign reversions in each of the three CD transitions. The data indicate that the verdin chromophore in **7, 1, 5** and **6** prefers the *P*-helicity conformation; whereas, in **2, 3** and **4** it prefers the *M*. The reason for the choice of helicity is not immediately obvious, but the preference is probably not strong because the CD magnitudes represent only  $\sim 5-10\%$  of the maximum  $\Delta\epsilon$  value

reported for verdins.<sup>2,10b</sup> Thus, the stereogenic centers at  $\beta, \beta'$ -positions in the propionic acid chains of **1-7** apparently exert only a small influence on the helical diastereoselectivity.

**TABLE 3.** Comparison of UV-Visible and Circular Dichroism Spectral Data for  $10^{-5}$  M ( $\beta S, \beta' S$ )-Dimethylmesobiliverdin-XIII $\alpha$  Cyclic Esters (**1-6**) and ( $\beta S, \beta' S$ )-Dimethylmesobiliverdin-XIII $\alpha$  Dimethyl Ester (**7**) in Chloroform and Methanol Solvents at 23°C.

Verdin	CHCl <sub>3</sub>				CH <sub>3</sub> OH			
	UV-Vis		CD		UV-Vis		CD	
	$\epsilon^{\max}$	( $\lambda^{\max}$ )	$\Delta\epsilon^{\max}$	( $\lambda^{\max}$ )	$\epsilon^{\max}$	( $\lambda^{\max}$ )	$\Delta\epsilon^{\max}$	( $\lambda^{\max}$ )
<b>1</b>	14700	(642)	+8.0	(637)	14300	(643)	+6.4	(639)
	51400	(367)	-23.6	(362)	51000	(363)	-23.8	(364)
	22500	(306)	+8.6	(299)	23100	(308)	+8.7	(297)
<b>2</b>	13800	(642)	-9.2	(630)	12900	(643)	-9.4	(641)
	47700	(369)	+25.5	(363)	47200	(364)	+21.4	(361)
	23300	(305)	-5.7	(300)	23500	(303)	-5.8	(298)
<b>3</b>	14300	(642)	-11.1	(642)	14100	(643)	-9.6	(631)
	50900	(369)	+34.5	(363)	51500	(364)	+30.5	(361)
	21300	(307)	-8.4	(298)	21700	(309) sh	-8.5	(297)
<b>4</b>	14700	(642)	-3.3	(649)	14400	(642)	-5.0	(647)
	52100	(369)	+6.6	(371)	52200	(365)	+12.5	(357)
	22300	(308)	< 0.5	(300)	22900	(312) sh	-3.1	(299)
<b>5</b>	14700	(644)	+11.8	(641)	14300	(646)	+3.5	(650)
	52100	(368)	-31.7	(364)	51900	(364)	-7.7	(362)
	22200	(308)	+8.5	(296)	22400	(308) sh	+3.3	(293)
<b>6</b>	13600	(640)	+7.7	(629)	13300	(644)	+8.0	(660)
	48700	(369)	-20.4	(364)	48800	(365)	-22.3	(363)
	21300	(307)	+4.8	(297)	21300	(310) sh	+5.7	(295)
<b>7</b>	14300	(644)	+6.1	(644)	13900	(644)	+4.1	(649)
	50000	(367)	-14.3	(365)	49900	(363)	-9.8	(364)
	24700	(304)	+2.5	(299)	24800	(310) sh	+1.4	(291)

**Conformational Analysis.** Analysis of verdin conformations has been discussed in detail by Falk.<sup>2</sup> Verdins possessing the natural, stable 4Z,10Z,15Z configuration, preferentially adopt either of two mirror image, helical porphyrin-like shapes, *M* and *P* (Fig. 1). The verdin *M* and *P* helical conformations lie at isoenergetic global minima and have an interconversion barrier of  $\sim 10$  kcal/mole.<sup>8</sup> Introduction of a methyl group at the *pro-S* site on the  $\beta$ -carbon of each propionic ester group (to give **7**) perturbs the *M*  $\rightleftharpoons$  *P* equilibrium. The ( $\beta S, \beta' S$ )-*M* diastereomer is not expected to have exactly the same total energy as the ( $\beta S, \beta' S$ )-*P*; however, it is not obvious by simple inspection which diastereomer is lower in energy. Molecular dynamics computations predict the ( $\beta S, \beta' S$ )-*P* to be more stable than the ( $\beta S, \beta' S$ )-*M*, and this prediction is in qualitative agreement with the CD spectral data (Table 3), where the positive long wavelength Cotton effect correlates with an excess of the *P*-helicity conformation.<sup>2</sup> On the basis of other work involving the bridged verdins of Fig. 2A,B and peptides of biliverdin,<sup>2,10</sup> one might predict that **7-P** would have  $\Delta\epsilon^{\max} \approx +240$  for the long wavelength CD transition. Consequently, the helical conformation selection imparted by the  $\beta S, \beta' S$  methyls is rather small (2-3%), suggesting an energy difference of  $< 100$  cal/mole.<sup>6</sup> The system is exquisitely sensitive to small perturbations by remote stereogenic centers.

When the propionic acid groups are linked as cyclic esters (Fig. 2C), even the smallest linkage ( $n=1$ ) does not distort the verdin helicity, as may be seen from the relevant torsion angles compared to those of mesobiliverdin-XIII $\alpha$  dimethyl ester and other "noncyclic" verdins (Table 4). However, conformational analysis of the cyclic esters is more complicated than the acyclic ester because the ester ring might be expected to alter the conformational energies and the activation barrier for  $M \rightleftharpoons P$  interconversion. In addition to the two enantiomeric helical verdin conformers ( $M$  and  $P$ ), one must consider enantiomeric cyclic ester ring helicities ( $m$  and  $p$ ). Thus, in mesobiliverdin-XIII $\alpha$  cyclic esters one finds a set of 4 diastereomers ( $mM$ ,  $pP$ ,  $mP$  and  $pM$ , Fig. 3) that are predicted to be nearly isoenergetic ( $\Delta\Delta H_f = 0.1$  kcal/mole). Three different interconversion pathways serve to connect the diastereomers: (1)  $mM \rightleftharpoons mP$  and  $pM \rightleftharpoons pP$ , (2)  $mM \rightleftharpoons pM$  and  $mP \rightleftharpoons pP$ , and (3)  $mM \rightleftharpoons pP$  and  $pM \rightleftharpoons mP$ . The barrier for (1) is predicted by molecular mechanics calculations<sup>7</sup> to be  $\sim 10.3$  kcal/mole; whereas, those for (2) and (3) are predicted to be prohibitively large. These data suggest that only two independent dynamic conformational equilibria are important (in Fig. 3:  $mM \rightleftharpoons mP$  and  $pM \rightleftharpoons pP$ ), and that while interconversion between  $M$  and  $P$  verdin helicity is feasible, interconversion between  $m$  and  $p$  ester ring helicity is not. One should, therefore, be able to separate the isomers belonging to the  $m$  and  $p$  manifolds, but this has not yet been accomplished.

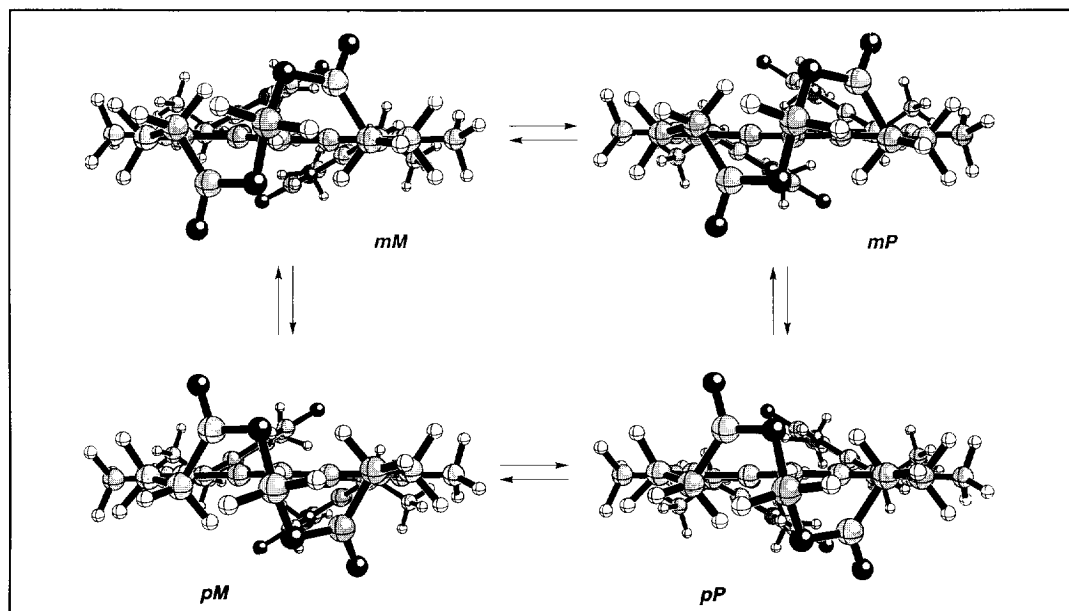


**FIGURE 3.** Ball and stick representations for the interconverting energy-minimized diastereomeric conformations of mesobiliverdin-XIII $\alpha$  methylene cyclic ester viewed from the  $-O-CH_2-O-$  ester unit toward C(10) of the verdin chromophore. An  $M$  or  $P$  helicity of the verdin chromophore can be recognized as can the ester ring helicity ( $m$  or  $p$ ). The horizontal equilibria pass over an  $M \rightleftharpoons P$  barrier of  $\sim 10$  kcal/mole, but the diastereomers cannot interconvert by vertical (or diagonal paths) as the  $m \rightleftharpoons p$  barrier is computed to be extremely high ( $\rightarrow \infty$ ).

Introduction of a methyl group at the  $\beta$  carbon in each propionic ester chain of the mesobiliverdin-XIII $\alpha$  methylene cyclic ester (Fig. 3) to form **1**, (of the Synthetic Scheme) lowers the  $M \rightleftharpoons P$  activation barrier from  $\sim 14$  to  $\sim 10$  kcal/mole. Similar energies are computed for **2-6** (Table 5).<sup>7</sup> In **1**, four well-defined stereois-

**TABLE 4.** Verdin Torsion Angles Computed by Molecular Mechanics<sup>a</sup>

Verdin	Torsion Angle (°) <sup>b</sup>						O(1)-O(19) Vertical Distance (Å) <sup>c</sup>
	21-4-5-6	4-5-6-22	22-9-10-11	9-10-11-23	23-14-15-16	14-15-16-24	
Biliverdin-IX $\alpha$ <sup>d</sup>	- 3.1	- 26.7	- 4.8	- 1.6	- 26.3	- 4.1	2.9
Mesobiliverdin-XIII $\alpha$ <sup>d</sup>	- 3.3	- 26.9	- 4.7	- 1.8	- 26.9	- 3.8	3.0
Mesobiliverdin-XIII $\alpha$ Dimethyl Ester <sup>d</sup>	- 3.5	- 27.2	- 4.8	- 1.9	- 26.6	- 3.7	3.0
Etiobiliverdin-IV $\gamma$ <sup>d</sup>	- 3.2	- 26.3	- 4.5	- 1.9	- 26.6	- 3.9	2.9
N <sub>21</sub> -N <sub>24</sub> -Methano- bridged Etiobiliverdin- IV $\gamma$ (Fig. 2A)	+8.9	+34.2	-47.2	-2.5	+13.7	+8.5	2.6
C <sub>2</sub> -C <sub>18</sub> Four Carbon Bridged Verdin (Fig. 2B) <sup>d</sup>	- 5.2	- 24.7	- 4.9	- 2.0	- 24.8	- 2.7	2.8
Mesobiliverdin-XIII $\alpha$ Methylene Cyclic Ester (Fig. 3) <sup>e</sup>	- 3.3	- 27.9	- 4.0	- 1.0	- 27.0	- 3.8	3.0

<sup>a</sup> Ref. 7. <sup>b</sup> See Fig. 2 for numbering. <sup>c</sup> The direct distance is 4.9-5.2 Å, except for entry 5, where it is 3.0 Å. <sup>d</sup> For *M*-helicity (Fig. 1A, B). <sup>e</sup> For *mM* or *pM*.

mers are found (Fig. 4A), with the *pM*  $\rightleftharpoons$  *pP* interconverting pair computed<sup>7</sup> to lie some 1.8-1.9 kcal below the *mP*  $\rightleftharpoons$  *mM* interconverting pair (Table 5). An extremely high *m*  $\rightleftharpoons$  *p* interconversion barrier separates the *m* and *p* manifolds ( $\rightarrow \infty$  kcal/mole), indicating that 1-6 consist of two pairs of interconverting diastereomers with no interconversion between the pairs. The relative stability of these isomer pairs is difficult to determine by inspection of molecular models (Fig. 4) but can be calculated by molecular mechanics.<sup>7</sup> In 1 it seems likely that the *p* diastereomers are lower energy than the *m*, but the ratio of *m* and *p* isomers actually present is unclear. Consequently, it is difficult to correlate the observed CD data (Table 3) with the calculated conformational energy differences data (Table 5). The former clearly indicate a (slight) predominance of the *P* helicity diastereomer(s), but the latter predict a slightly more stable *M* diastereomer with *p* ester ring helicity. The calculated energies do not include solvent molecules, which might play a role in reversing the order of stability predicted in Table 5.

Interestingly, cyclic esters 2, 3 and 4 exhibit CD Cotton effect sign reversals (Table 3) compared with 1 and 5-7, suggesting that the *M*-helicity verdin conformation(s) are more stable than *P*. Again, the CD intensities are weak, and it is not easy to rationalize the slightly greater stability of the *M* conformer(s) of, *e.g.*, 2, from inspection of molecular models or molecular graphics (Fig. 4B). In 2 and 3, the *m*-helicity ester

**TABLE 5.** Molecular Dynamics Computed<sup>a</sup> Relative Heats of Formation ( $\Delta H_f$ ) of ( $\beta S, \beta' S$ )-Dimethylmesobiliverdin-XIII $\alpha$  Cyclic Esters (1-6) and the Parent Acyclic Ester ( $\beta S, \beta' S$ )-Dimethylmesobiliverdin-XIII $\alpha$  Dimethyl Ester (7).

Ester Ring Helicity	Verdin Tetrapyr- role Helicity	Relative $\Delta\Delta H_f$ (kcal/mole) for Ester Diastereomers						
		1	2	3	4	5	6	7
<i>m</i>	<i>M</i>	1.88	0.05	0.05	0.99	0.00	0.41	3.29 <sup>b</sup>
<i>m</i>	<i>P</i>	1.77	0.00	0.00	0.86	0.43	0.00	0.00 <sup>b</sup>
<i>p</i>	<i>M</i>	0.00	0.01	1.35	0.00	4.02	1.03	—
<i>p</i>	<i>P</i>	0.22	0.75	1.63	1.07	2.77	1.40	—
<i>M</i> $\rightleftharpoons$ <i>P</i> Barrier <sup>c</sup>		9.7	9.8	11.8	8.4	9.9	10.0	10.2

<sup>a</sup> SYBYL ver. 6.0. <sup>b</sup> Acyclic, no ester ring helicity. <sup>c</sup> Interconversion barrier, kcal/mole.



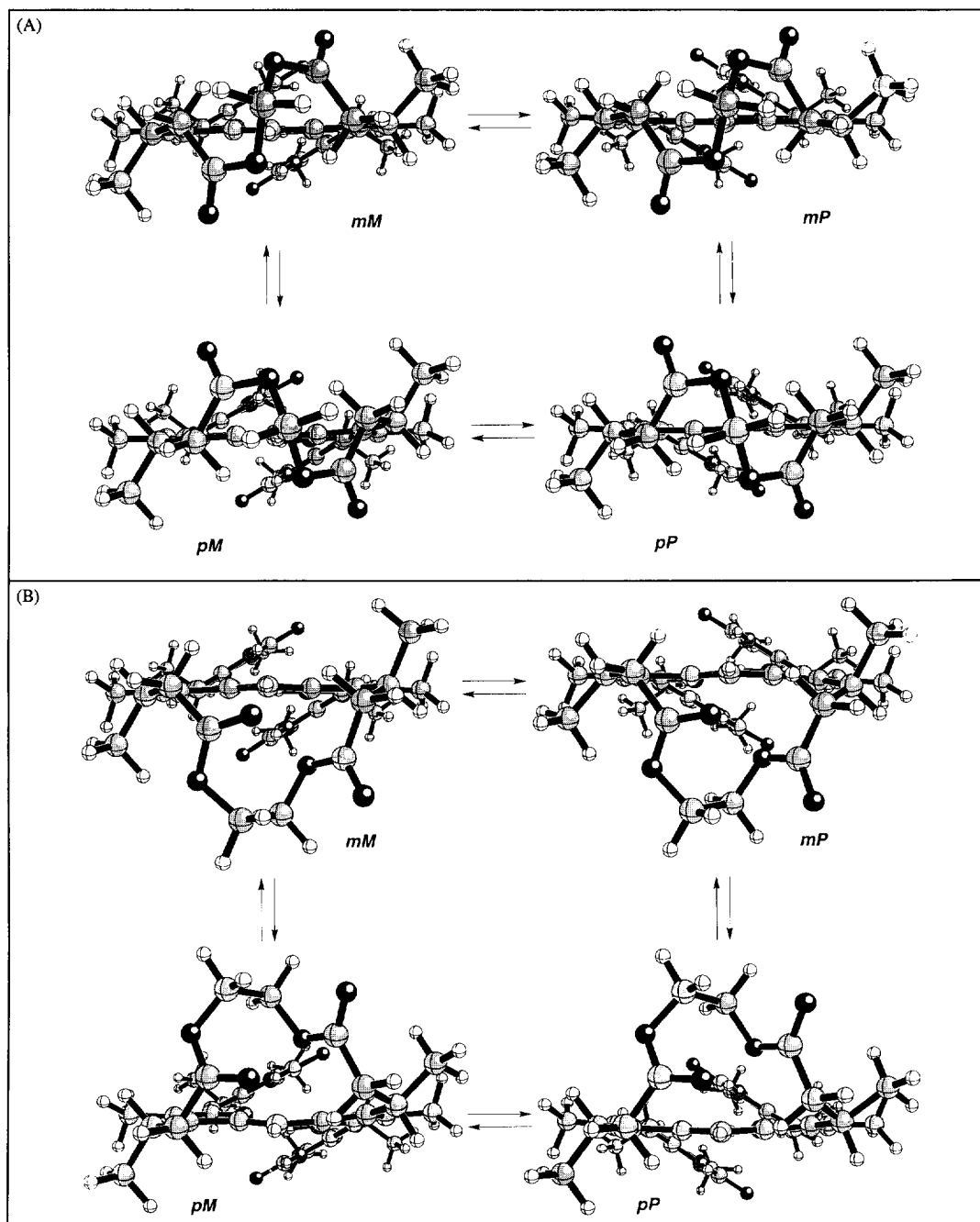


**FIGURE 4.** Ball and stick representations for interconverting the energy-minimized diastereomeric conformations of the  $n=1$  and  $n=2$  cyclic esters of  $(\beta S, \beta' S)$ -dimethylmesobiliverdin-XIII $\alpha$ , **1** (A) and **2** (B), respectively. The horizontal equilibria pass over barriers of  $\sim 10$  kcal/mole; the vertical equilibria can be neglected, as the barriers  $\rightarrow \infty$ .

ring conformations are slightly preferred, but in **4**, the *p* is preferred. As with **1**, it is difficult to rationalize the CD data from the predicted energy differences of Table 5 — except perhaps in **4**, where the *pM* diastereomer is predicted to be 0.86–1.07 kcal/mole more stable than any others. Curiously, the Cotton effect signs, which reversed when the ester belt was expanded by one  $-\text{CH}_2-$  unit (in going from **1** to **2**) and remain invariant as the number of  $-\text{CH}_2-$  units increased from 2 to 4, are found to reverse again when the  $(-\text{CH}_2)_n$  belt is expanded by one more  $-\text{CH}_2-$  (in going from  $n=4$  (**4**) to  $n=5$  (**5**)).

### SUMMARY

Linking the propionic acid groups of mesobiliverdin through  $(-\text{CH}_2)_n$  chains ( $n=1-6$ ) imposes no unusual distortion in the verdin chromophore skeleton. Conformational analysis of the cyclic esters, which takes into account the intrinsic *M* and *P* verdin helicity as well as the helicity (*m* and *p*) of the cyclic ester suggests the presence of 4 diastereomers: *mM*, *mP*, *pM* and *pP*. Molecular mechanics calculations indicate a low barrier ( $\sim 10$  kcal/mole) to *M*  $\rightleftharpoons$  *P* interconversion and a very high barrier ( $\rightarrow \infty$ ) to *m*  $\rightleftharpoons$  *p* interconversion. Optically active ( $\beta S, \beta' S$ )-dimethylmesobiliverdin-XIII $\alpha$  dimethyl ester (**7**) shows a weakly positive long wavelength CD Cotton effect, indicating a slight excess of the *P*-helicity conformer — as predicted by molecular mechanics calculations. Verdin cyclic esters **1**, **5** and **6** also exhibit weakly positive long wavelength CD Cotton effects, suggesting a predominance of the *mP* or *pP* diastereomers. In contrast, verdin cyclic esters **2**, **3** and **4** show weakly negative long wavelength Cotton effects, indicating a slight predominance of *mM* and/or *pM* diastereomers. The energy differences are small, and molecular mechanics is less useful in rationalizing the observed CD data. The failure is probably due to neglect of solvent.

### EXPERIMENTAL

**General Procedures.** All ultraviolet-visible spectra were recorded on a Perkin Elmer model 3840 diode array or Cary 219 spectrophotometer, and all circular dichroism (CD) spectra were recorded on a Jasco J-600 instrument. NMR-spectra were obtained on a GE QE-300 or GN-300 300 MHz spectrometer in  $\text{CDCl}_3$  solvent and reported in  $\delta$  ppm upfield from  $(\text{CH}_3)_4\text{Si}$ . For  $^{13}\text{C}$ -NMR spectra, the J-modulated spin-echo experiment (Attached Proton Test) was used. Optical rotations were measured in chloroform on a Perkin Elmer model 141 polarimeter. Mass spectra (EI) were measured on a Finnigan MAT SSQ 710 instrument. Melting points were determined on a Mel-Temp capillary apparatus and are uncorrected. Combustion analyses were carried out by Desert Analytics, Tucson, AZ. Analytical thin layer chromatography was carried out on J.T. Baker silica gel IB-F plates ( $125\mu$  layer). Radial chromatography was carried out on Merck silica gel 60 PF<sub>254</sub> with  $\text{CaSO}_4$  preparative thin layer grade, using a Chromatotron (Harrison Research, Inc., Palo Alto, CA).

Spectral data were obtained in spectral grade solvents (Aldrich or Fisher). Dimethylsulfoxide (Fisher) was dried and distilled from calcium hydride. Methanol was dried and distilled from magnesium methoxide, and tetrahydrofuran (THF) was dried and distilled from lithium aluminum hydride. Diiodomethane, 1,2-dibromoethane, 1,3-dibromopropane, 1,4-dibromobutane, 1,5-dibromopentane, 1,6-dibromohexane, and cesium carbonate were from Aldrich.

**(4Z,10Z,15Z)-8,12-Bis(methoxycarbonyl-( $\beta S$ )-methylene)-3,17-diethyl-2,7,13,18-tetramethyl-1,19,21,24-tetrahydrobilin-1,19-dione [( $\beta S, \beta' S$ )-Dimethylmesobiliverdin-XIII $\alpha$  dimethyl ester] (**7**). Optically pure ester was prepared as described earlier,<sup>14</sup> and has mp 212–216°C and  $[\alpha]_{436}^{20} -3480$  ( $c 1.6 \times 10^{-3}$ ,  $\text{CHCl}_3$ ).**

**( $\beta S, \beta' S$ )-Dimethylmesobiliverdin-XIII $\alpha$  (**8**). Optically pure **7** (482 mg, 0.75 mmol) was dissolved in a mixture of 225 mL of tetrahydrofuran:methanol (1:1 by vol), both  $\text{N}_2$  saturated. To the solution was added ascorbic acid (225 mg) and 0.2 M aqueous NaOH (225 mL,  $\text{N}_2$  saturated). The mixture was stirred under  $\text{N}_2$  at 50°C for 5 h. After cooling to room temperature, 100 mL of water and 100 mL of chloroform were**

added. The colorless organic layer was discarded, and the aqueous layer was slowly acidified at 0°C with 10% HCl. The desired blue product was extracted with CHCl<sub>3</sub> (4 x 100 mL), washed with water (2 x 600 mL), and the solvent was removed under vacuum. Residual moisture was removed azeotropically with dry benzene, and 425 mg (92%) of blue-green solid (**8**) was obtained after drying under vacuum over P<sub>2</sub>O<sub>5</sub>. It was used directly in the next step.

**(βS,β'S)-Dimethylmesobiliverdin-XIIIα Dicesium Salt (9)**. Diacid **8** (123 mg, 0.2 mmol) was dissolved under N<sub>2</sub> in 15 mL of methanol and 10-20 mL of THF until a homogeneous solution was obtained. A solution of 72 mg (0.22 mmol) of cesium carbonate in 2 mL of water was added, and the mixture was stirred for 30 min. The solvents were removed completely under vacuum (0.5 mm Hg, 40°C), and the solid residue (**9**) was dried for 48 h under vacuum over P<sub>2</sub>O<sub>5</sub>; then, it was used directly in the following to prepare cyclic esters **1-6**.

**General procedure for synthesis of cyclic esters of (βS,β'S)-dimethylmesobiliverdin-XIIIα**. Dicesium salt **9** (0.2 mmol) was dissolved in 100 mL of freshly distilled, dry (CH<sub>3</sub>)<sub>2</sub>SO under N<sub>2</sub>. Then a freshly prepared solution of 1.00 mmole of α,ω-dihaloalkane in 40 mL of dry (CH<sub>3</sub>)<sub>2</sub>SO was delivered to it through a septum, in 4 equal portions using a syringe pump. Each aliquot was delivered over an 8 h period, while the solution was stirred magnetically at room temperature, and the solution was stirred for 40 h after each addition. The total reaction time was 8 days. The mixture was diluted with 300 mL of CHCl<sub>3</sub>, washed with water (4 x 300 mL), dried over anhyd. Na<sub>2</sub>SO<sub>4</sub> and filtered. The solvent was removed under vacuum, and the resulting crude product was purified by radial chromatography on silica gel, eluting with 1.5-2.5% CH<sub>3</sub>OH in CH<sub>2</sub>Cl<sub>2</sub> and collecting only fractions containing the bright blue major nonpolar band.

**(βS,β'S)-Dimethylmesobiliverdin-XIIIα Methylene Cyclic Ester (1)** was obtained from **9** and diiodomethane in 62% yield and had mp 268-271°C (decomp.) and [α]<sub>436</sub><sup>20</sup> -4980 (*c* 1.7 x 10<sup>-3</sup>, CHCl<sub>3</sub>). Mass spectral molec wt. calcd. for C<sub>36</sub>H<sub>42</sub>N<sub>4</sub>O<sub>6</sub>: 626. Found *m/z* (rel. abund.): 626 [M<sup>+</sup>•] (100%).

*Anal.* Calcd. for C<sub>36</sub>H<sub>42</sub>N<sub>4</sub>O<sub>6</sub> · CH<sub>3</sub>OH (658.8): C, 67.45; H, 7.04; N, 8.50.  
Found: C, 67.79; H, 6.64; N, 8.33.

**(βS,β'S)-Dimethylmesobiliverdin-XIIIα Ethylene Cyclic Ester (2)** was obtained from **9** and 1,2-dibromoethane in 67% yield and had mp 272-274°C and [α]<sub>436</sub><sup>20</sup> +5340 (*c* 1.4 x 10<sup>-3</sup>, CHCl<sub>3</sub>). Mass spectral molec wt. calcd. for C<sub>37</sub>H<sub>44</sub>N<sub>4</sub>O<sub>6</sub>: 640. Found *m/z* (rel. abund.): 640 [M<sup>+</sup>•] (100%).

**(βS,β'S)-Dimethylmesobiliverdin-XIIIα Propylene Cyclic Ester (3)** was obtained in 66% yield from **9** and 1,3-dibromopropane and had mp 292-294°C and [α]<sub>436</sub><sup>20</sup> +6330 (*c* 2.0 x 10<sup>-3</sup>, CHCl<sub>3</sub>). Mass spectral molec wt. calcd. for C<sub>38</sub>H<sub>46</sub>N<sub>4</sub>O<sub>6</sub>: 654. Found *m/z* (rel. abund.): 654 [M<sup>+</sup>•] (100%).

**(βS,β'S)-Dimethylmesobiliverdin-XIIIα Tetramethylene Cyclic Ester (4)** was obtained from **9** and 1,4-dibromobutane in 88% yield and had mp 276-279°C and [α]<sub>436</sub><sup>20</sup> +1340 (*c* 1.7 x 10<sup>-3</sup>, CHCl<sub>3</sub>). Mass spectral molec wt. calcd. for C<sub>39</sub>H<sub>48</sub>N<sub>4</sub>O<sub>6</sub>: 668. Found *m/z* (rel. abund.): 668 [M<sup>+</sup>•] (100%).

**(βS,β'S)-Dimethylmesobiliverdin-XIIIα Pentamethylene Cyclic Ester (5)** was obtained in 66% yield from **9** and 1,5-dibromopentane and had mp 316-319°C (decomp.) and [α]<sub>436</sub><sup>20</sup> -6150 (*c* 2.1 x 10<sup>-3</sup>, CHCl<sub>3</sub>). Mass spectral molec wt. calcd. for C<sub>40</sub>H<sub>50</sub>N<sub>4</sub>O<sub>6</sub>: 682. Found *m/z* (rel. abund.): 682 [M<sup>+</sup>•] (100%).

**(βS,β'S)-Dimethylmesobiliverdin-XIIIα Hexamethylene Cyclic Ester (6)** was obtained from **9** and 1,6-dibromohexane in 50% yield and had mp 286-288°C (decomp.) and [α]<sub>436</sub><sup>20</sup> -4360 (*c* 1.7 x 10<sup>-3</sup>, CHCl<sub>3</sub>). Mass spectral molec wt. calcd. for C<sub>41</sub>H<sub>52</sub>N<sub>4</sub>O<sub>6</sub>: 696. Found *m/z* (rel. abund.): 696 [M<sup>+</sup>•] (100%).

**Acknowledgement.** We thank the National Institutes of Health (HD 17779) for generous support of this work. D.T.A. is a Wilson Fellowship Awardee. S.E.B. is on leave from the Institute of Organic Chemistry, Bulgarian Academy of Sciences, Sofia.

## REFERENCES AND NOTES

- (1) McDonagh, A.F. "Bile Pigments: Bilatrienes and 5,15-Biladienes" in *The Porphyrins* (Dolphin, D., Ed.) Academic Press: New York, Vol VI, chap. 6, **1979**.
- (2) Falk, H. *The Chemistry of Linear Oligopyrroles and Bile Pigments*; Springer Verlag: New York, Vienna, **1989**.
- (3) Gossauer, A. *Chimia* **1994**, *48*, 352-361.
- (4) For leading references, see Ostrow, J.D., ed., *Bile Pigments and Jaundice*; Marcel-Dekker: New York, **1986**.
- (5) (a) Fischer, H.; Plieninger, H. *Naturwiss.* **1942**, *30*, 382-387.  
(b) Fischer, H.; Plieninger, H. *Z. Physiol. Chem.* **1942**, *274*, 231-260.
- (6) (a) Sheldrick, W.S. *J. Chem. Soc. Perkin Trans. II* **1976**, 1457-1462.  
(b) Wagner, U.; Kratky, C.; Falk, H.; Wöss, H. *Monatsh. Chem.* **1991**, *122*, 749-758.  
(c) Lehner, H.; Braslavsky, S.E.; Schaffner, K. *Angew. Chem.* **1978**, *90*, 1012-1013.  
(d) Takahashi, H.; Kuroyanagi, K.; Yamada, O.; Kaneko, N. *Chem. Phys. Lett.* **1983**, *94*, 38-40.  
(e) Meyer, E.F. Jr.; Pépe, G. *Am. Cryst. Assoc. Ser. 2* **1979**, *6*, 93.
- (7) Molecular mechanics calculations and molecular modelling was carried out on an Evans and Sutherland ESV-10 workstation using version 6.0 of SYBYL (Tripos Assoc., St. Louis, MO). [See Person, R.V.; Peterson, B.R.; Lightner, D.A. *J. Am. Chem. Soc.* **1994**, *116*, 42-59.] The ball and stick drawings were created from the atomic coordinates of the molecular dynamics structures using Müller and Falk's "Ball and Stick" program (Cherwell Scientific, Oxford, U.K.) for the Macintosh.
- (8) Lehner, H.; Riemer, W.; Schaffner, K. *Liebig's Ann. Chem.* **1979**, 1798-1801.
- (9) Falk, H.; Thirring, K. *Tetrahedron* **1981**, *37*, 761-766.
- (10) (a) Krois, D.; Lehner, H. *J. Chem. Soc. Perkin Trans. II* **1993**, 1351-1360.  
(b) Krois, D.; Lehner, H. *J. Chem. Soc. Perkin Trans. II* **1993**, 1837-1839.
- (11) Ribó, J.M.; Crusats, J.; Marco, M. *Tetrahedron* **1994**, *50*, 3967-3974.
- (12) Huber, R.; Schneider, M.; Mayr, I.; Müller, K.; Deutzmann, R.; Suter, F.; Zuber, H.; Falk, H.; Kayser, H. *J. Mol. Biol.* **1987**, *198*, 499-513.
- (13) Krois, D.; Lehner, H. *Monatsh. Chem.* **1991**, *122*, 89-100.
- (14) Boiadjiev, S.E.; Person, R.V.; Puzicha, G.; Knobler, C.; Maverick, E.; Trueblood, K.N.; Lightner, D.A. *J. Am. Chem. Soc.* **1992**, *114*, 10123-10133.

(Received in USA 6 February 1995)